

Fabrication of PU/PEGMA crosslinked hybrid scaffolds by in situ UV photopolymerization favoring human endothelial cells growth for vascular tissue engineering

Heyun Wang · Yakai Feng · Bo An ·
Wencheng Zhang · Minglin Sun · Zichen Fang ·
Wenjie Yuan · Massuri Khan

Received: 18 November 2011 / Accepted: 7 March 2012 / Published online: 20 March 2012
© Springer Science+Business Media, LLC 2012

Abstract Poly(ethylene glycol) methacrylate (PEGMA) was introduced into a polyurethane (PU) solution in order to prepare electrospun scaffold with improving the biocompatibility by electrospinning technology for potential application as small diameter vascular scaffolds. Crosslinked electrospun PU/PEGMA hybrid nanofibers were fabricated by a reactive electrospinning process with *N,N'*-methylenebisacrylamide as crosslinker and benzophenone as photoinitiator. The photoinduced polymerization and

crosslinking reaction took place simultaneously during the electrospinning process. The electrospinning solutions with various weight ratios of PU/PEGMA were successfully electrospun. No significant difference in the scaffold morphology was found by SEM when PEGMA content was <20 wt%. The crosslinked fibrous scaffolds of PU/PEGMA exhibited higher mechanical strength than the pure PU scaffold. The hydrophilicity of scaffolds was controlled by varying the PU/PEGMA weight ratio. The tissue compatibility of electrospun nanofibrous scaffolds were tested using human umbilical vein endothelial cells (HUVECs). Cell morphology and cell proliferation were measured by SEM, fluorescence microscopy and thiazolyl blue assay (MTT) after 1, 3, 7 days of culture. The results indicated that the cell morphology and proliferation on the crosslinked PU/PEGMA scaffolds were better than that on the pure PU scaffold. Furthermore, the appropriate hydrophilic surface with water contact angle in the range of 55–75° was favorable of improvement the HUVECs adhesion and proliferation. Cells seeded on the crosslinked PU/PEGMA (80/20) scaffolds infiltrated into the scaffolds after 7 days of growth. These results indicated the crosslinked electrospun PU/PEGMA nanofibrous scaffolds were potential substitutes for artificial vascular scaffolds.

H. Wang · Y. Feng (✉) · Z. Fang · W. Yuan · M. Khan
School of Chemical Engineering and Technology, Tianjin
University, Tianjin 300072, China
e-mail: yakaifeng@hotmail.com

H. Wang
China School of Chemistry and Chemical Engineering, Shihezi
University, Shihezi 832002, China

Y. Feng
Key Laboratory of Systems Bioengineering of Ministry of
Education, Tianjin University, Tianjin 300072, China

Y. Feng
Joint Laboratory for Biomaterials and Regenerative Medicine,
Tianjin University, Weijin Road 92, Tianjin 300072, China

Y. Feng
Helmholtz-Zentrum Geesthacht, Kantstr. 55, 14513 Teltow,
Germany

B. An · M. Sun
Department of Orthopedics, Affiliated Hospital of Logistics
University of Chinese People's Armed Police Force, Tianjin
300072, China

W. Zhang
Department of Physiology and Pathophysiology, Logistics
University of Chinese People's Armed Police Force, Tianjin
300072, China

1 Introduction

Polyurethanes (PUs), with excellent elasticity and mechanical properties, have been widely applied in many fields of materials, especially in the field of biomedical materials [1, 2]. PUs have better biocompatibility than other synthetic polymers because of the micro-phase separated structure [3, 4]. However, the poor hydrophilicity and hemocompatibility of PUs become the bottleneck when

they are applied in tissue engineering [5]. As we all know, the scaffolds should have moderate hydrophilicity which can be in favor of cell attachment and proliferation [6]. Oligomers made of poly(ethylene glycol) methacrylate, PEGMA, have exhibited a desired properties in the production of biomaterials and been often used as a hydrophilic polymer for surface modification [7]. PEGMA could be grafted onto biomaterial surfaces and provide a biocompatibility layer which could reduce the absorption of plasma albumen and red blood cell [8, 9], because of its characteristics of hydrophilicity, large exclusion volume, and unique coordination with surrounding water molecules in an aqueous medium [10]. Moreover, it has unique properties of nontoxicity and nonimmunogenicity, which are very important for biomaterials [11, 12]. However, because of its high solubility in water, it was necessary to attach it to a polymeric surface or to crosslink it in the form of a network. Until now, photocrosslinked PEG-based materials have been fabricated by spin-coating of photosensitive macromer and UV exposure, but due to the process, the surface area is limited. If its biocompatible properties are combined with the advantages of high surface-to-volume ratio of nanofibers, these materials could be more efficient supports for enzyme and cell immobilization for biocatalysis, sensing, or tissue engineering [13, 14].

Taking into consideration the fact, electrospinning technology is an inexpensive, effective and simple method to produce nanofibrous mats from both synthetic and natural polymers. It had gained increased interest in tissue engineering, which could produce polymer fibers with diameter ranging from few nanometers to microns [15, 16]. Electrospun membranes possess high porosity, large surface area and maximum interconnectivity of pores with a non-woven nanofibrous structure [17–19]. The fibers within the resulting scaffold more closely mimic the size and structure of the native extracellular matrix than other previously investigated scaffolds, which can lead to beneficial cellular interactions [20, 21].

In this paper, we aimed to develop an in situ method to prepare the crosslinked PU/PEGMA nanofibers by electrospinning technology in which the photopolymerization of oligomers was carried out during this process. To the best of my knowledge, the crosslinked PU/PEGMA fibrous scaffold by in situ photopolymerization has not previously been reported. Combining the fiber fabrication process with photochemical reactions enabled the polymerization and crosslinking of hydrophilic materials while they were produced into the nanofibrous form [22]. The possibility of employing the crosslinked PU/PEGMA hybrid scaffolds as a vascular graft is investigated and discussed. The results demonstrated the feasibility of electrospinning of a photocross linkable macromers and provided a foundation for further optimization of engineered fibrous tissues.

2 Materials and methods

2.1 Materials

PU (Chronoflex AL 80A) with a number average molecular weight of 110,000 was purchased from Cardio International Incorporated, USA. PEGMA ($M_n = 400$) was purchased from Aldrich. *N,N'*-Methylenebisacrylamide (MBAm) and benzophenone (BP) were received from Aladdin reagent Inc. Dissolving solvents of *N,N'*-dimethylformamide (DMF) and tetrahydrofuran (THF) were products from sigma. All other chemical solvents were of analytical grade without further purification.

2.2 Preparation of crosslinked electrospun PU/PEGMA scaffolds

Figure 1 showed the schematic electrospinning in situ UV photopolymerization process. Firstly, PU was dissolved in the mixture solvent of DMF and THF with 1:1 volume ratio to obtain a PU solution of 10 % (w/v). A mixture of PEGMA, MBAm as crosslinker and BP as photoinitiator was prepared with the following weight ratio (wt%): PEGMA:MBAm:BP = 97.5:2.0:0.5. Then mixed solutions of PU/PEGMA with the different weight ratios (PU/PEGMA: 90/10, 80/20, 70/30, 60/40, 50/50) were prepared. The mixed polymer solutions were placed into a 10 mL plastic syringe with a 25 gauge (inner diameter 0.25 mm) capillary tip. The flow rate (0.6 mL/h) of PU/PEGMA solutions was controlled using a syringe pump. The positive lead from a high voltage supply was attached by an alligator clip to the external surface of the metal syringe needle. The electrospinning voltage (18 kV) was supplied. A grounded steel plate located 20 cm away from the tip of the syringe needle was used to collect the nanofiber scaffolds. The UV light from a 200 W Hg lamp was irradiated directly on to the jet traveling from the needle to the collector. Upon UV irradiation (200 W Hg arc lamp), the photoinitiator in the jet initiates further polymerization and cross-linking of unreacted monomers and oligomers while the jet is traveling to the collector.

2.3 Characterization

2.3.1 Morphology

The nanofibrous morphologies were investigated with scanning electron microscopy (SEM, Hitachi S-3400N, Japan). Based on the SEM images, the fiber average diameter and standard deviations were analyzed using an image analysis program (Adobe Photoshop 7.0).

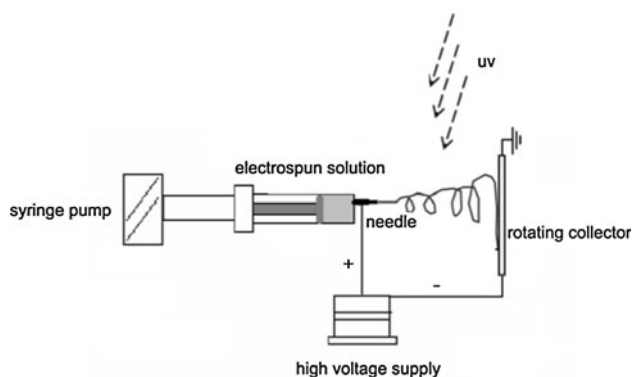


Fig. 1 Schematic illustration of electrospinning equipment

2.3.2 ATR-FTIR analyze

The surface chemistry of the scaffolds was characterized by attenuated total reflectance Fourier transform infrared spectrometer (ATR-FTIR, Bio-Rad FTS-6000, USA). The transmittance of each sample was recorded between 4,000 and 500 cm^{-1} with a resolution of 2 cm^{-1} .

2.3.3 DSC measurement

The residual methacrylic functional groups were determined by residual enthalpy of reaction by differential scanning calorimetry (DSC) measurement [23]. BP was added the mixed electrospinning solution as a photoinitiator. Then the mixed solution was exposed UV light for different time intervals to generate crosslinked samples with varying degrees of polymerization. A DSC scan was successively performed using Mettler-Toledo TA3000 instrument with 0–250 $^{\circ}\text{C}$ heating run at rate with 10 $^{\circ}\text{C}/\text{min}$. The residual heat of polymerization was measured by integration of the exothermal peak at 120 $^{\circ}\text{C}$. These values were compared to the total enthalpy of polymerization (previously determined in purely thermal polymerization experiments) obtaining the extent of reaction or conversion polymerization.

$$\text{Conversion } \% = \frac{(\Delta H_{tot} - \Delta H_{res})}{\Delta H_{tot}}, \quad (1)$$

where ΔH_{tot} was the total enthalpy of polymerization and ΔH_{res} was the residual enthalpy of polymerization.

The melting and crystallization characteristics of the crosslinked PU/PEGMA hybrid scaffolds were investigated by means of DSC (Perkin-Elmer system, USA). DSC measurements were carried out using a Perkin-Elmer system with a heating or cooling rate of 10 $^{\circ}\text{C}/\text{min}$, under temperature ranging from -50 to 100 $^{\circ}\text{C}$ and under constant N_2 stream (30 mL/min). About 5–8 mg of sample was used for each measurement, and an empty aluminum pan was used as a reference.

2.3.4 Tensile tests

The mechanical behavior of the electrospun scaffolds was investigated with a tensile machine (M350-20KN, Testmetric, UK) equipped with a 100 N load cell at a cross-head speed of 10 mm/min in the ambient environment. All the data reported for the tensile modulus, tensile strength, and elongation at break represented average results of six tests and were analyzed statistically by the method of the *t* test.

2.3.5 Water contact angle measurements

To evaluate the hydrophilic/hydrophobic properties of the crosslinked PU/PEGMA scaffolds, the water contact angle was examined. The samples were cut into a rectangular shape (15 $\text{mm} \times 8 \text{ mm}$). The contact angle was measured by the sessile drop method using a video contact angle instrument (KrussEasyDrop goniometer, Germany) at room temperature. The contact angle was calculated with the AutoFAST algorithm within the image analysis software.

2.3.6 Water uptake measurement

In order to determine the water uptake of crosslinked PU/PEGMA scaffolds, samples were prepared by being completely dried with a vacuum oven. The dried samples were weighed and subsequently immersed in a 15 mL conical tube with distilled water. After 1 h of immersion, the samples were taken and weighed after removing the surface water with filter paper. The water uptake (%) was calculated as follows:

$$\text{Water uptake } (\%) = \left[\frac{(w_t - w_o)}{w_o} \right] \times 100\%, \quad (2)$$

where w_o was the weight of scaffolds before dissolving and w_t was the weight of the scaffolds after dissolving.

2.4 In vitro cell culture

Human umbilical vein endothelial cells (HUVECs, Tianjin Hospital of Armed Police Forces, Tianjin, China) were cultured at 37 $^{\circ}\text{C}$ in a humidified atmosphere of 5 % CO_2 in air, in 25 cm^2 tissue culture flasks containing 5 mL Dulbecco's modified Eagle medium (DMEM, Gibco, USA) supplemented with 10 % newborn calf serum (Gibco), 50 U/mL penicillin and 50 U/mL streptomycin. Following trypsin treatment, the cells were detached from the flasks and monolayers were prepared by seeding HUVECs on gelatin-precoated culture plates and incubated for 24–48 h until confluent. Cells up to the fourth passage were used for all experiments.

2.5 Cell seeding and morphology observation

For in vitro culture adhesion and morphology studies, the crosslinked PU/PEGMA scaffolds were cut into 12 mm diameter circles. The prepared scaffolds were sterilized by being soaked in 75 % ethanol for 30 min and then washed thoroughly by phosphate buffered saline (PBS) (Sigma Aldrich, St. Louis, MO). To provide a hydrophilic surface conducive for efficient cell attachment, scaffolds were pre-wetted by immersion in cell culture medium for 24 h in the 37 °C incubator. HUVECs grown in 25 cm² cell culture flasks were trypsinized, counted, and plated at a density of 5×10^4 cells/cm² onto the surface of pre-wetted scaffolds that were placed in 24-well culture plates. In order to prevent the scaffolds from floating, thin glass rings adapted to the inner diameter of the wells were used. Cellular scaffolds were incubated at 37 °C for 4 h to allow HUVECs to diffuse into and adhere to the scaffold before the addition of 1 mL of medium to each well. During the initial 4 h of incubation, 40 µL of culture medium was applied to each cellular scaffold every 30 min to prevent desiccation of the constructs.

After 1, 3 and 7 days culture, the crosslinked PU/PEGMA nanofibrous scaffolds were harvested, washed with PBS to remove the non-adherent cells and then fixed in 2.5 % glutaraldehyde for 2 h at room temperature, and then dehydrated through a series of graded alcohol solutions from 50 to 100 % in steps of 10 % for 10 min each. After dehydration, samples were lyophilized for 3 days. All samples were sputter coated with gold before SEM observation. SEM images were captured on both HUVECs-scaffolds and bare scaffolds at an accelerating voltage of 10 kV.

2.6 Fluorescence assay

HUVECs was stained cells with Hoechst 33342 and propidium iodide (PI, Sigma, St. Louis, MO, USA). Nonfluorescent cell-permanent Ho. 33342 is enzymatically converted to intense blue fluorescent calcein in live cells, while PI enters cells with damaged membranes, binding to nucleic acids, and producing a bright red fluorescence in dead cells. Cell-scaffold constructs were rinsed, incubated in 500 µg/mL Ho. 33342 and 500 µg/mL PI solution diluted with PBS for 10 min at 37 °C. Scaffolds were then imaged using the inverted fluorescent Microscope (Olympus CKX41). Cell counting data were generated from counting total number of cells (PI/Ho. 33342 stained) in three separate fiber pieces per time point. A minimum of 10 randomly selected visual fields (at $\times 20$ magnification in a fluorescent microscope were counted per fiber piece. The total number of live and dead cells was counted at three different time points (day 1, 3, and 7 of co-culture and differentiation) and was presented as number of cells per

day of culture. The results are presented as mean \pm standard deviation. Data were analyzed using Student's *t* test. $p < 0.05$ was considered statistically significant.

2.7 MTT assay

After HUVECs were cultured in 96-well plate for 1, 3 and 7 days, the thiazolyl blue assay (MTT, Sigma, St. Louis, MO) assay was used to determine the proliferation rate of HUVECs. Scaffolds were cut into 5 mm diameter circles, then sterilized and pre-wetted as above shown. HUVECs were plated at a density of 5×10^4 cells/cm² onto the surface of scaffolds that were placed in 96-well culture plates. After cells were cultured for 1, 3 and 7 days, the MTT assay was used to determine the proliferation rate of cells. 20 µL of MTT (5 mg/mL) was added to each well and incubated at 37 °C for 4 h in humidified atmosphere of 5 % CO₂ in air. At the end of the assay, the purple formazan reaction product was dissolved by adding 150 µL dimethyl sulfoxide (DMSO) and vibrated slightly for 10 min, then 100 µL solution was transferred to a new 96-well plate. The solution of each sample was placed in a microtiter plate (Bio-Rad Laboratories) and the absorbance was measured at 490 nm.

2.8 Histology

To quantify the extent of cellular infiltration, scaffolds were removed from media at the appropriate time points and fixed in 4 % paraformaldehyde solution overnight. They were then soaked in a 20 % sucrose solution for 4 h, then exchanged in a 30 % sucrose solution overnight. Scaffolds were embedded in SAKURA Tissue-TeK embedding medium (USA) and snap frozen in liquid nitrogen. The resulting blocks were cut into 20 µm sections using a Leica CM1850 Cryostat, and mounted onto Superfrost/Plus microscope slides (Fisher Scientific). To visualize cellular nuclei and cytoplasm, the sections were stained with hematoxylin and eosin dyes. Images were then taken using Olympus microscope (CX21) and analyzed using MiE V2.0 software.

3 Results and discussion

3.1 SEM morphology of crosslinked electrospun PU/PEGMA scaffolds

Because PEGMA was a low molecular weight oligomer, PEGMA content should influence the solution properties and the morphology of electrospun hybrid nanofibers. Figure 2 demonstrated the SEM micrographs of electrospun crosslinked PU/PEGMA fibers. With increasing

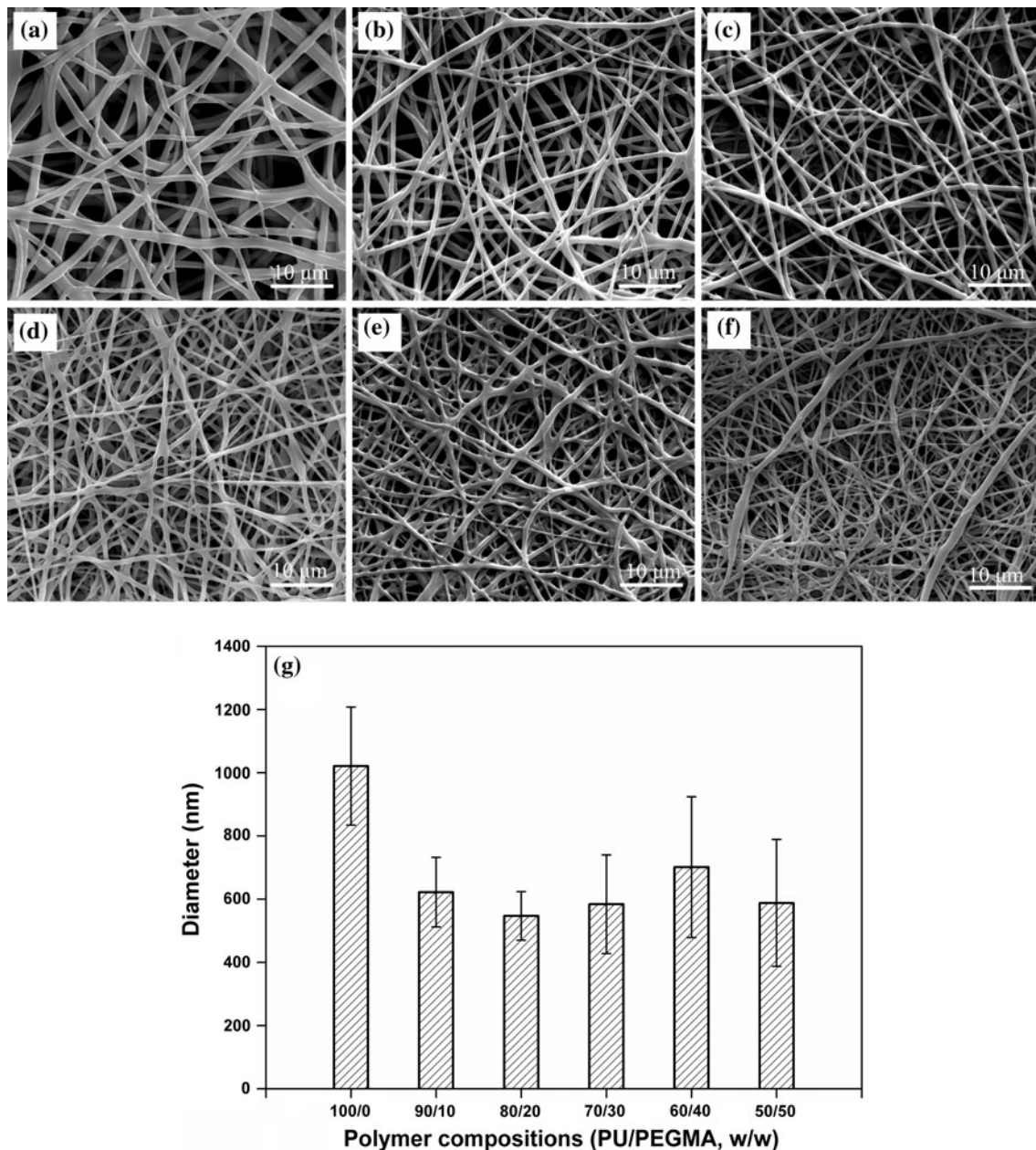


Fig. 2 SEM micrographs and fiber diameters of crosslinked electrospun PU/PEGMA fibrous scaffolds with different PU/PEGMA weight ratios: **a** 100/0, **b** 90/10, **c** 80/20, **d** 70/30, **e** 60/40, **f** 50/50, and **g** average fiber diameters of crosslinked electrospun PU/PEGMA fibrous scaffolds

PEGMA content, the viscosity of electrospinning solutions decrease owing to the dilution of PEGMA [24]. The electrospun fibers changed from fine fibers to bonded fibers as shown in Fig. 2. When PU/PEGMA was 90/10 and 80/20, uniform fibrous scaffolds with average fiber diameter of 622 ± 110 nm and 547 ± 77 nm were obtained (Fig. 2g). The fine morphology of electrospun fibers could be well preserved in despite of PEGMA photopolymerization. However, when the PEGMA weight ratio exceeded 30 wt%, the electrospun fibers became non-uniform with distortion. Furthermore, many fibers were fused together

and some thick fibers formed a web-like fiber morphology. The negative effect of the PEGMA on the PU electrospinning behavior could be caused by the reduced chain entanglement due to lowering PU concentration in spinning solution which further exhibited the decrease in fiber diameter and increased defects with PEGMA amount. During the reactive electrospinning process, most of solvent in the fibers was volatilized, but PEGMA mainly remained on the surface of the fibers. With a small amount of PEGMA (10 wt%) in the fibers, UV photopolymerization happened instantly inside and on the surface of electrospun

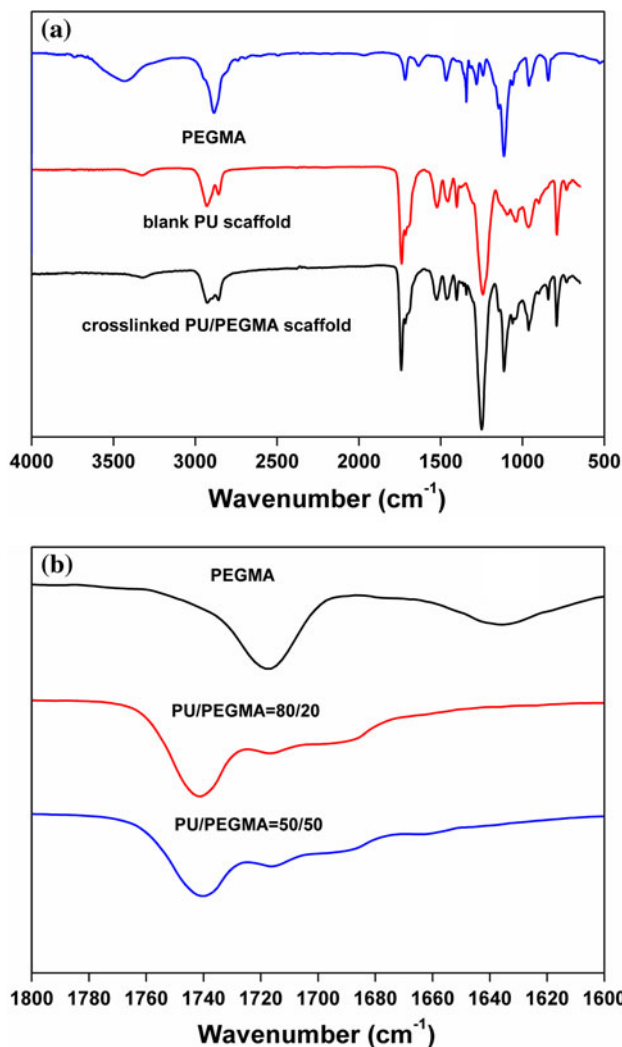


Fig. 3 ATR-FTIR of macromonomer PEGMA, electrospun PU scaffold and crosslinked electrospun PU/PEGMA scaffold **a** wavenumber: 500–4,000 cm^{-1} and **b** wavenumber: 1,600–1,800 cm^{-1}

fibers. When PEGMA content was above 20 wt%, PEGMA took part in the formation of fibers during the electrospinning process, also adhered onto the fiber surface. Thus, fibers distorted and even fused to form very thick fibers.

3.2 ATR-FTIR

Figure 3a demonstrated the ATR-FTIR spectra of PU, macromonomer PEGMA and crosslinked PU/PEGMA hybrid scaffolds. The peaks at 2,952 and 2,853 cm^{-1} corresponded to the antisymmetric and symmetrical stretching vibration peaks of $-\text{CH}_2-$ in PU scaffold. The absorption peaks at 1,731 and 1,521 cm^{-1} were responsible for the carbonyl and C–N bonds, respectively. The peak at 1,468 cm^{-1} was a symmetry bending vibration peak of $-\text{CH}_2-$. The band at 1250 cm^{-1} was assigned to the ester C–O–C stretching in the polycarbonate segments. It could

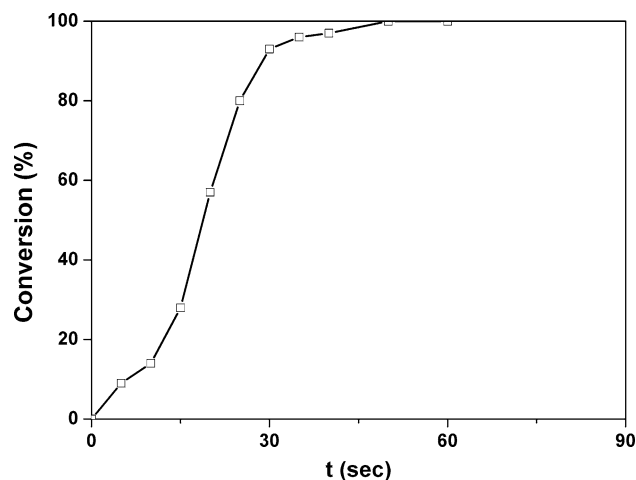


Fig. 4 Conversion versus of hybrid PU/PEGMA solution of polymerization obtained by DSC

be obviously observed the intensity of stretching vibration peak of C=O at 1,731 cm^{-1} and C–O at 1,242 cm^{-1} were significantly reinforced in crosslinked PU/PEGMA hybrid scaffold due to the addition of PEGMA. Particularly, characteristic peaks of the ether bond at 848 and 1,101 cm^{-1} strongly evidenced that hybrid PU/PEGMA scaffold was fabricated. Figure 3b showed the ATR-FTIR spectra of electrospun PU/PEGMA scaffolds with different weight ratios of PEGMA generated through UV photopolymerization. The C=C bond at 1,638 cm^{-1} disappeared completely proving the absence of double bonds within the hybrid scaffolds after the UV irradiation process. This fact indicated that the semi-interpenetrating polymer network within the PU fiber scaffolds had been formed successfully.

3.3 PEGMA photopolymerization and thermal analysis

The kinetic of photopolymerization of crosslinked PEGMA polymers was studied by DSC testing. The procedure was based on the estimation of the residual heat of polymerization (ΔH_{res}) after UV exposure. After measuring the total heat of polymerization ΔH_{tot} in a separate DSC experiment based on photoinitiator, the conversion at various stages of photopolymerization was calculated by Eq. 1. Figure 4 showed conversion versus time of polymerization data by the DSC measurement. It could be observed the crosslinked reaction of PEGMA could nearly completed around 30 s and no residual methacrylic functional groups were found in the hybrid PU/PEGMA solutions. Furthermore, Differential scanning calorimetry was also used to investigate the morphology the crosslinked polymer phase in the hybrid fibrous scaffolds. DSC scans for hybrid scaffolds were shown in Fig. 5, along with PEGMA oligomers as comparison. The result indicated that PEGMA oligomers had a broad melting process ranging from -21 to 8 $^{\circ}\text{C}$ on

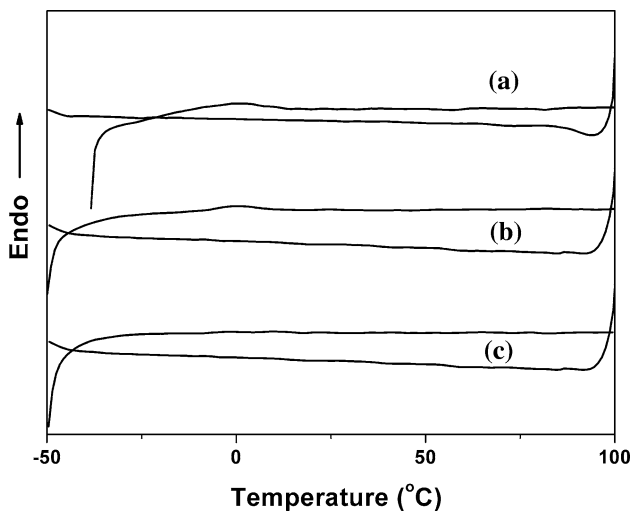


Fig. 5 DSC scans for *a* macromonomer PEGMA, *b* no crosslinked PU/PEGMA (70/30) fibrous scaffold, *c* crosslinked PU/PEGMA (70/30) fibrous scaffold. In each case, the *upper curve* was on heating and the *lower curve* was cooling

heating and no crystallization on cooling process. For the no crosslinked PU/PEGMA hybrid scaffold, the melting process remained at a higher temperature than that of PEGMA oligomers, although reduced in enthalpy, and no crystallization on cooling process was found similar with the PEGMA oligomers. Interestingly, melting process was eliminated in the crosslinked PU/PEGMA hybrid scaffolds, indicating that the crosslinked PEGMA phase in PU matrix was completely amorphous.

3.4 Mechanical properties

In the reactive electrospinning process, PEGMA molecules can react with crosslinker (MBAm) to generate a network structure that could penetrate into PU macromolecules to form a semi-interpenetrating network. The network structure was confirmed by FTIR and DSC measurements. It was hypothesized that the fibrous structure of electrospun PU scaffolds combined with the crosslinking network of PEGMA would possibly give rise to new electrospun scaffolds with improved mechanical properties [25]. Mechanical behaviors of the crosslinked electrospun PU/PEGMA scaffolds with the different weight ratio showed in Fig. 6. Without PEGMA, the electrospun PU scaffold had an elastic modulus of 1.43 ± 0.03 MPa, a tensile strength of 2.04 ± 0.17 MPa, and an elongation at break of 136 ± 32 %. The crosslinked electrospun PU/PEGMA scaffolds demonstrated mechanical behavior like that of rubber, in that stress–strain curves showed linear elasticity as their intrinsic material property. Generally, the mechanical properties of the electrospun scaffolds depended on the inherent material character and geometric arrangement, which contributed to

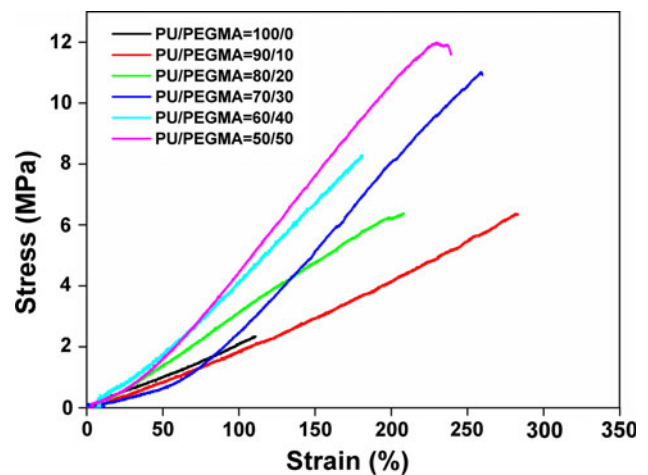


Fig. 6 Mechanical behaviors of the crosslinked electrospun PU/PEGMA scaffolds with different weight ratios of PU/PEGMA

the most important adhered and tangled effect of fibers [26]. Hence, PEGMA formed crosslinked netlike inner fiber structure of PU through photopolymerization also enhanced the action of fibers through adhered each other. When the weight ratio of PU/PEGMA decreased from 90/10 to 50/50, the tensile strength and elongation at break of crosslinked PU/PEGMA scaffold changed from 5.98 ± 0.72 MPa, 285 ± 27 % to 12.04 ± 0.87 MPa, 234 ± 19 %, respectively. The results attributed to the covalent bonds between PEGMA inside fibers and chemical bonding of the fiber junctions. Therefore, it was obviously suggested that the crosslinking photopolymerization of PEGMA oligomers could enhanced the tensile properties significantly.

3.5 Wettability and water absorption capability of crosslinked PU/PEGMA scaffolds

Hydrophilicity was one of the most important factors that affected the cytocompatibility of biomaterials [27]. The adhesion and growth of cells on a surface were considered to be strongly influenced by the balance of hydrophilicity/hydrophobicity, frequently described as wettability [27–29]. Many studies had demonstrated that cells adhere, spread and grow more easily on moderately hydrophilic substrates than on hydrophobic or very hydrophilic ones [28, 29]. To investigate the effect of PEGMA content on the wettability of the crosslinked PU/PEGMA nanofibrous scaffolds, the water contact angle and water uptake measurements were performed and illustrated in Fig. 7. It could be observed that the pure PU scaffold had the highest contact angle values at $118.8^\circ \pm 7.8^\circ$ among all scaffolds, and the contact angle values decreased with the increase content of PEGMA. When the weight ratio of PEGMA increased up to 50 wt%, the contact angle decreased to about $20.2^\circ \pm 2.3^\circ$. The results revealed that the addition of PEGMA

changed the hydrophobicity of hybrid PU/PEGMA scaffolds. When the content of PEGMA was less than 10 wt%, the hydrophobic surface were detected. It was attributed to the combined effects of methyl group enrichment on the fiber surface and surface roughness of the electrospun scaffolds [30]. When the content of PEGMA increased and exceeded 20 wt%, the contact angle decreased significantly. The hydrophilicity of the scaffolds based on PU was improved by addition of higher content PEGMA. The water uptake property of scaffolds could facilitate cellular nutrient supply and waste removal [31]. The water uptake capacity of pure PU scaffold was about 42 ± 4.3 %, and far lower than that of the hybrid scaffolds with PEGMA. The water uptake ratio of hybrid scaffolds ranged from 60.71 ± 5.1 to 122 ± 8.8 % when the weight ratio of PEGMA was increased from 10 to 50 wt%. Ji et al. [32] found a similar trend in blending PLA/PEG scaffolds; the increased PEGMA weight ratio resulted in enhanced the water uptake capacity.

3.6 Cell morphology

As the potential vascular grafts for tissue engineering applications, the abilities of cell adhesion and proliferation on scaffold surface are very important, commonly, the scaffold must have an interconnected pore network structure for cell attaching and in-growth [33, 34]. Therefore, in this study, HUVECs were seeded on the surface of the crosslinked PU/PEGMA fibrous scaffolds and cultured for 3 days to investigate the cell morphology. After cultured for 72 h, the cell morphology was observed by SEM and presented in Fig. 8. It could be found that HUVECs could adhere and grow on the surfaces of all scaffolds, adhered closely on the nanofibrous surfaces and stretched out along the fibers. The cells attached on the crosslinked PU/PEGMA hybrid scaffolds were more than those of pure PU scaffold. The cells adhered approximately 5 % area on the hydrophobic PU nanofibrous scaffold. These cells were only clustered together and stretched across the randomly interconnected structures. When the content of PEGMA increased to 20 and 30 wt%, the adhered cells significantly increased in number, and covered more than 40–50 % area of the fibrous scaffolds. Also the cells reached out pseudopodia along the fibrous direction and formed a continuous monolayer. On the other hand, comparing the cell morphology on the hybrid scaffold with different content of PEGMA, it could be obviously seen that the attachment and growth of cells on scaffolds with lower content of PEGMA (20 and 30 wt%) were better than higher content of PEGMA (40 and 50 wt%). It is well known that initial cell adhesion could be affected by the surface hydrophilicity of scaffolds [35, 36]. Surface wettability of artificial materials is one of the most important factors determining cell

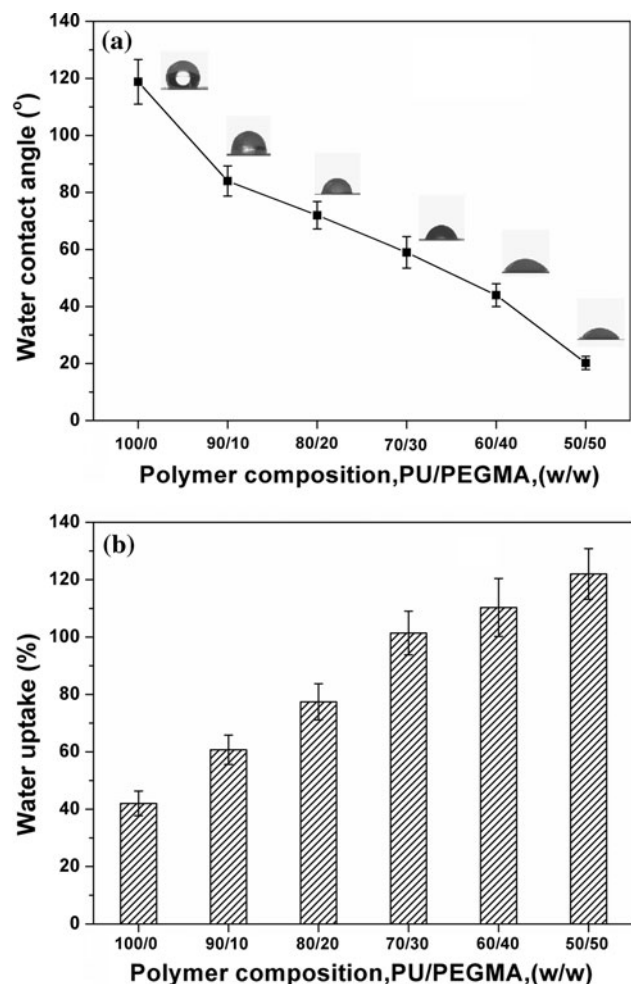


Fig. 7 Water contact angle (a) and water uptake (b) of crosslinked PU/PEGMA fibrous scaffolds with the different weight ratios of PU/PEGMA

adhered behavior. Cells attach and proliferate less well on surfaces having wettability which was too low or too high [37]. From Fig. 8, it can be inferred that HUVECs could grow well on the appropriate hydrophilic surface with the water contact angle in the range of 55–75° which was favorable of improvement the cell adhesion and growth.

3.7 Viability of the HUVECs

The death rates of HUVECs populations on crosslinked PU/PEGMA (80/20) scaffolds were 1.74 ± 0.21 % on day 1, 1.38 ± 0.19 % on days 3 and 1.17 ± 0.11 % on days 7, respectively. These low death rates in the initial stage of HUVECs culturing showed that the scaffolding materials were highly biocompatible, without invoking any cytotoxic effects, and that the surface biochemistry is favorable for cell attachment, which is critical for endothelial cell survival [38]. Illustrated in Fig. 9, it showed that cells could adhere and spread on the surface of the crosslinked

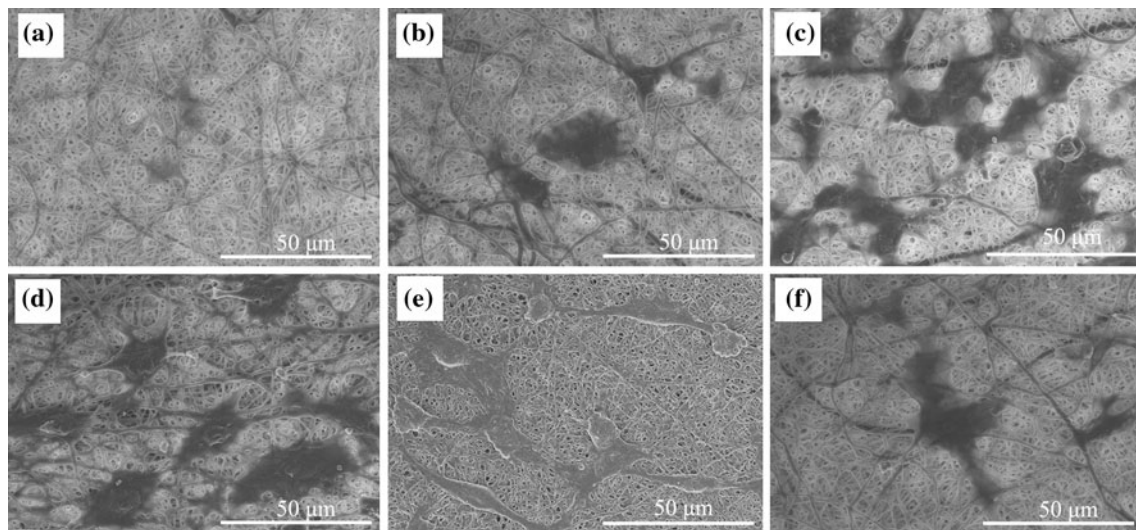


Fig. 8 SEM images of HUVECs cultured on fibrous scaffolds with the different weight ratios of crosslinked PU/PEGMA scaffolds. **a** PU/PEGMA (100/0), **b** PU/PEGMA (90/10), **c** PU/PEGMA (80/20), **d** PU/PEGMA (70/30), **e** PU/PEGMA (60/40), **f** PU/PEGMA (50/50)

PU/PEGMA (80/20) hybrid scaffold, and the cell density on day 7 was much higher than that of day 1 and day 3. HUVECs spread not only in large number but also distribute evenly on the crosslinked PU/PEGMA nanofibrous scaffolds after 1, 3, and 7 days of culture. The coverage and morphology revealed by the SEM and fluorescent images testified that the crosslinked PU/PEGMA scaffolds possessed necessary biochemical properties to recruit endothelial cells onto its surface and provides a favorable biophysical environment for the endothelial regeneration.

3.8 Proliferation of the HUVECs

The incorporation of PEGMA improved the hydrophilicity of crosslinked PU/PEGMA hybrid scaffolds. Generally, hydrophobic surfaces could absorb more proteins in the first step to provide a better cell adhesion environment [39]. However, the cell proliferation performed different behavior. The proliferation HUVECs on the crosslinked PU/PEGMA hybrid scaffolds was evaluated by the MTT

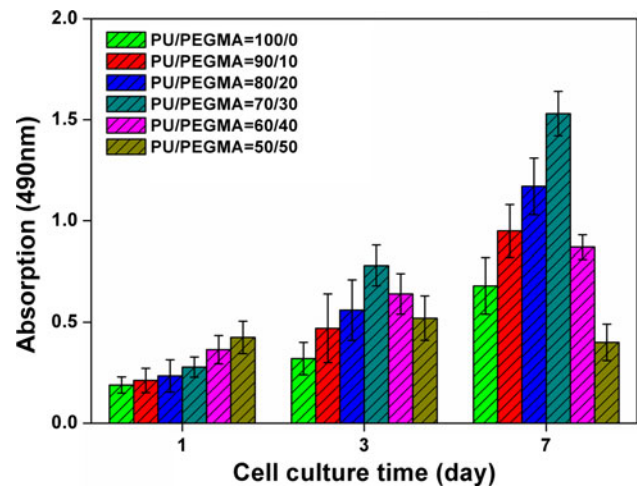


Fig. 10 Proliferation of HUVECs cells on crosslinked PU/PEGMA nanofibrous scaffolds. Cells were seeded at a density of 5×10^4 cells/cm² and cultured for a period of 7 days. Data are representative of three independent experiment and all data points plotted as mean \pm SD ($n = 3$)

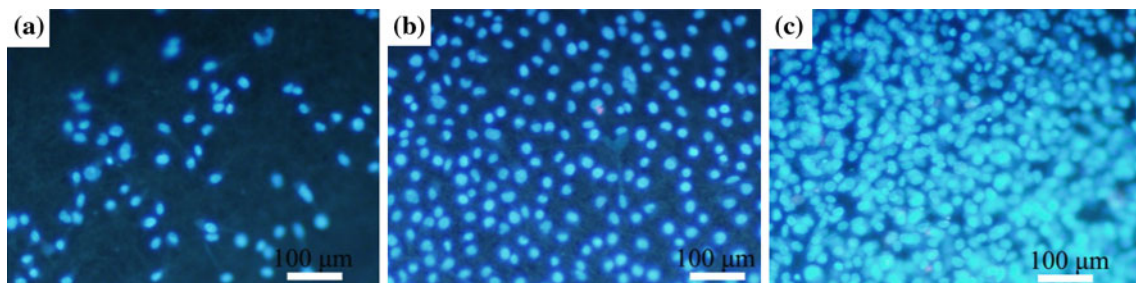


Fig. 9 Live/dead cells staining fluorescent images of HUVECs cultured on the crosslinked PU/PEGMA scaffolds (PU/PEGMA = 80/20). The live cells are stained blue and the dead cells

red. **a** For 1 day of culture ($\times 20$ magnification), **b** 3 days of culture ($\times 20$ magnification), **c** 7 days of culture ($\times 20$ magnification). The images were captured directly on an inverted fluorescent microscope

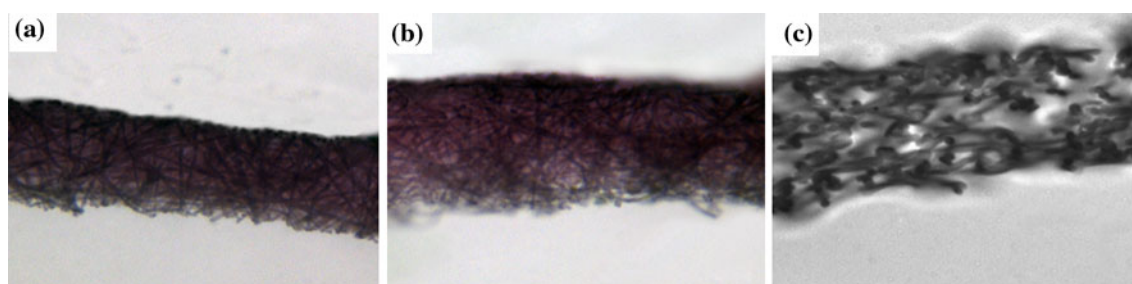


Fig. 11 Images of H&E stained sections of the crosslinked PU/PEGMA (PU/PEGMA = 80/20) scaffolds seeded with HUVECs after **a** 1 day, **b** 3 days and **c** 7 days show that there is a progressive

infiltration and growth into the scaffolds throughout the 7 days. For all images, section thicknesses = 20 μm , $\times 100$ magnification

assay with 1, 3 7 culture days. As shown in Fig. 10, the HUVECs on all scaffolds adhered to some extent and began to proliferate after culturing for 1 day, but there were no significant differences between the cell number on the PU scaffolds and that on the crosslinked PU/PEGMA hybrid scaffolds ($p > 0.05$). The results indicated that the electrospun scaffolds were able to support HUVECs proliferation without producing toxic effects. After culturing for 3 and 7 days, the cell number on the crosslinked PU/PEGMA hybrid scaffolds increased quickly. The cell proliferation on the hybrid scaffolds showed the higher proliferation rate than that on pure PU scaffold, and the HUVECs on the crosslinked PU/PEGMA (70/30) hybrid scaffolds exhibited the highest proliferation rate. It might be attributed that the PEGMA on the nanofibrous surface had been gradually exclude out the medium during the culturing process after the initial inhibition period, thus enhanced the cell growth and proliferation on the scaffolds [40]. As PEGMA content was up to 50 wt%, it could be observed the cell proliferation rate was lowest in all scaffolds. The reason might be that hybrid scaffolds became better hydrophilic, and which could cause reduced protein absorption and consequently delayed the cell adhesion and proliferation. In our studies, the cell culture experiments indicated the appropriate content of PEGMA in the hybrid scaffolds was able to promote the cell proliferation, and the one with PU/PEGMA (70/30) might furnish a favorable biophysical housing for endothelial regeneration.

3.9 In vitro cell infiltration studies

It has been suggested that the pore size of a scaffold should be at least 10 μm to support cell infiltration [41]. On 1 day, a small number of HUVECs had attached to the surface of the crosslinked PU/PEGMA (80/20) scaffold, and their infiltration was limited to the top surface (Fig. 11a). By day 3, a large number of the cells had concentrated on the surface of scaffolds, but less had infiltrated deeply into the scaffolds (Fig. 11b). Furthermore, by day 7, cells were found throughout the scaffold at a depth of 20 μm from the

surface, and the number of cells had increased tremendously, both near the surface and deep within the scaffold (Fig. 11c). This result demonstrates that the scaffolds of crosslinked PU/PEGMA (80/20) by in situ photopolymerization could form large three-dimensional pores to support high cell infiltration.

4 Conclusions

Crosslinked PU/PEGMA hydrophilic nanofibrous scaffolds were fabricated directly from PU and PEGMA macromonomer solutions by reactive electrospinning method. The crosslinked PU/PEGMA (90/10, 80/20) uniform fibrous scaffolds were obtained with the average fiber diameter of 622 ± 110 and 547 ± 77 nm. A small amount PEGMA could improve the mechanical properties of electrospun PU scaffolds effectively, while fiber morphology could be preserved well. Furthermore, HUVECs were cultured onto the crosslinked PU/PEGMA scaffolds, the results were found that the cells attached, survived and proliferated significantly better compared with the PU scaffold. This new approach confirmed the advantages offered by the crosslinked PU/PEGMA hybrid scaffolds in providing appropriate mechanical properties combining with good cytocompatibility. Combining PU with the hydrophilic PEGMA polymer through a reactive electrospinning process could provide a potential substitute for artificial vascular scaffolds.

Acknowledgments This work has been financially supported by Program for New Century Excellent Talents in University “NCET”, Ministry of Education of P. R. China, and by the International Cooperation from Ministry of Science and Technology of China (Grant No. 2008DFA51170).

References

1. Feng YK, Zhang SF, Zhang L, Guo JT, Xu YS. Synthesis and characterization of hydrophilic polyester-PEO networks with shape-memory properties. *Polym Adv Technol*. 2010;79:1431–9.

2. Zhao HY, Feng YK, Guo JT. Grafting of poly(ethylene glycol) monoacrylate onto polycarbonate urethane surfaces by ultraviolet radiation grafting polymerization to control hydrophilicity. *J Appl Polym Sci*. 2011;119:3717–27.
3. Zhang SF, Feng YK, Zhang L, Guo JT, Xu YS. Biodegradable polyester urethane networks for controlled release of aspirin. *J Appl Polym Sci*. 2010;116(2):861–7.
4. Feng YK, Xue Y, Guo JT, Cheng L, Jiao LC, Zhang Y, Yue JL. Synthesis and characterization of poly(carbonate urethane) networks with shape-memory properties. *J Appl Polym Sci*. 2009;112: 473–8.
5. Klee D, Hocker H. Polymers for biomedical applications: improvement of the interface compatibility. *Adv Polym Sci*. 1999;149:1–57.
6. Horbett TA, Waldburger JJ, Ratner BD, Hoffman AS. Cell adhesion to a series of hydrophilic–hydrophobic copolymers studies with a spinning disc apparatus. *J Biomed Mater Res*. 1988; 22:383–404.
7. Kim SH, Kim SH, Nair SJ, Moore E. Reactive electrospinning of cross-linked poly(2-hydroxy ethyl methacrylate) nanofibers and elastic properties of individual hydrogel nanofibers in aqueous solutions. *Macromolecules*. 2005;38:3719–23.
8. Kim SE, Heo DN, Lee JB, Kim JR, Park SH, Jeon SH, Kwon IK. Electrospun gelatin/polyurethane blended nanofibers for wound healing. *Biomed Mater*. 2009;4:1–11.
9. Damodaran VB, Fee CJ, Ruckh T, Popat KC. Conformational studies of covalently grafted poly(ethylene glycol) on modified solid matrices using x-ray photoelectron spectroscopy. *Langmuir*. 2010;26:7299–306.
10. Altankov G, Thom V, Groth T, Jankova K, Jonsson G, Ulbricht M. Modulating the biocompatibility of polymer surfaces with poly(ethylene glycol): effect of fibronectin. *J Biomed Mater Res*. 2000;52:219–30.
11. Tziampazis E, Kohn J, Moghe PV. PEG-variant biomaterials as selectively adhesive protein templates: model surfaces for controlled cell adhesion and migration. *Biomaterials*. 2000;21: 511–20.
12. Efremova NV, Sheth SR, Leckband DE. Protein-induced changes in poly(ethylene glycol) brushes: molecular weight and temperature dependence. *Langmuir*. 2001;17:7628–36.
13. Tan AR, Ifkovits JL, Baker BM, Brey DM, Mauck RL, Burdick JA. Electrospinning of photocrosslinked and degradable fibrous scaffolds. *J Biomed Mater Res*. 2008;87:1034–43.
14. Choi SS, Hong JP, Seo YS, Chung SM, Nah C. Fabrication and characterization of electrospun polybutadiene fibers crosslinked by UV irradiation. *J Appl Polym Sci*. 2006;101:2333–7.
15. Kidoaki S, Kwon IK, Matsuda T. Mesoscopic spatial designs of nano and microfiber meshes for tissue-engineering matrix and scaffold based on newly devised multilayering and mixing electrospinning techniques. *Biomaterials*. 2005;26:37–46.
16. Vaz CM, Tuijl SV, Bouten CVC, Baaijens FPT. Design of scaffolds for blood vessel tissue engineering using a multi-layering electrospinning technique. *Acta Biomater*. 2005;1:575–82.
17. Jin Y, Yang DZ, Zhou YS, Ma GP, Nie J. Photocrosslinked electrospun chitosan-based biocompatible nanofibers. *J Appl Polym Sci*. 2008;109:3337–43.
18. Courtney T, Sacks M, Stankus S. Design and analysis of tissue engineering scaffolds that mimic soft tissue mechanical anisotropy. *Biomaterials*. 2006;27:3631–8.
19. Lee KH, Kim HY, La YM, Lee DR, Sung NH. Influence of a mixing solvent with tetrahydrofuran and *N,N*-dimethyl formamide on electrospun poly(vinyl-chloride) nonwoven mats. *J Polym Sci B*. 2002;40:2259–68.
20. Xu F, Cui FZ, Jiao YP, Meng QY, Wang XP, Cui XY. Improvement of cytocompatibility of electrospinning PLLA microfibers by blending PVP. *J Mater Sci Mater Med*. 2009;20: 1331–8.
21. Li WJ, Jiang YJ, Tuan RS. Chondrocyte phenotype in engineered fibrous matrix is regulated by fiber size. *Tissue Eng*. 2006;12: 1775–85.
22. Wang L, Topham PD, Mykhaylyk OO, Howse JR, Bras W, Jones RAL, Ryan AJ. Electrospinning pH-responsive block copolymer nanofibers. *Adv Mater*. 2007;19:3544–8.
23. Turri S, Levi M, Emilietri E, Surinao R, Bongiovanni R. Direct photopolymerisation of PEG-methacrylate oligomers for an easy prototyping of microfluidic structures. *Macromol Chem Phys*. 2010;211:879–87.
24. Zhao L, Zhang H, Li XR, Zhao J, Zhao C, Yuan XY. Modification of electrospun poly(vinylidene fluoride-cohexafluoropropylene) membranes through the introduction of poly(ethylene glycol) dimethacrylate. *J Appl Polym Sci*. 2009;111:3104–12.
25. Zheng XF, Yang F, Wang SG, Lu SB, Zhang WG, Liu SY, Huang JX, Wang AY, Yin BS, Ma N, Zhang L, Xu WJ, Guo QY. Fabrication and cell affinity of biomimetic structured PLGA/articular cartilage ECM composite scaffold. *J Mater Sci Mater Med*. 2011;22:693–704.
26. Choi WS, Bae JW, Lim HR, Joung YK, Park JC, Kwon IK, Park KD. RGD peptide-immobilized electrospun matrix of polyurethane for enhanced endothelial cell affinity. *Biomed Mater*. 2008;3:4104–12.
27. Wang YQ, Cai JY. Enhanced cell affinity of poly(L-lactic acid) modified by base hydrolysis: wettability and surface roughness at nanometer scale. *Curr Appl Phys*. 2007;7:108–11.
28. Webb K, Hlady V, Tresco PA. Relative importance of surface wettability and charged functional groups on NIH 3T3 fibroblast attachment, spreading, and cytoskeletal organization. *J Biomed Mater Res*. 1998;41:422–30.
29. Ertel SI, Ratner BD, Horbett TA. Radiofrequency plasma deposition of oxygen-containing films on polystyrene and poly(ethylene terephthalate) substrates improves endothelial cell growth. *J Biomed Mater Res*. 1990;24:1637–59.
30. Ma ML, Hill RM, Lowery JL, Fridrikh SV, Rutledge GC. Electrospun poly(styrene-block-dimethylsiloxane) block copolymer fibers exhibiting superhydrophobicity. *Langmuir*. 2005;21:5549–54.
31. Hoffman AS. Hydrogels for biomedical applications. *Ann NY Acad Sci*. 2001;944:62–73.
32. Ji CD, Annabi N, Hosseinkhani M, Sivaloganathan S, Dehghani F. Fabrication of poly-D,L-lactide/polyethylene glycol scaffolds using the gas foaming technique. *Acta Biomater*. 2012;8:570–8.
33. Thomas V, Dean DR, Jose MV, Mathew B, Chowdhury S, Vohra YK. Nanostructured biocomposite scaffolds based on collagen coelectrospun with nanohydroxyapatite. *Biomacromolecules*. 2007;8:631–7.
34. Li WJ, Laurencin CT, Catterson EJ, Tuan RS, Ko FK. Electrospun nanofibrous structure: a novel scaffold for tissue engineering. *J Biomed Mater Res*. 2002;60:613–21.
35. Zhang X, Thomas V, Xu YY, Bellis SL, Vohra YK. An in vitro regenerated functional human endothelium on a nanofibrous electrospun scaffold. *Biomaterials*. 2010;31:4376–81.
36. Nam J, Huang Y, Agarwal S, Lannutti J. Improved cellular infiltration in electrospun fiber via engineered porosity. *Tissue Eng*. 2007;13:2249–57.
37. Arima Y, Iwata H. Effect of wettability and surface functional groups on protein adsorption and cell adhesion using well-defined mixed self-assembled monolayers. *Biomaterials*. 2007;28:3074–82.
38. Meng ZX, Wang YS, Ma C, Zheng W, Li L, Zheng YF. Electrospinning of PLGA/gelatin randomly-oriented and aligned nanofibers as potential scaffold in tissue engineering. *Mater Sci Eng C*. 2010;30:1204–10.

39. Wang BY, Fu SZ, Ni PY, Peng JR, Zhang L, Luo F, Liu H, Qian ZY. Electrospun polylactide/poly(ethylene glycol) hybrid fibrous scaffolds for tissue engineering. *J Biomed Mater Res A*. 2011; 100A:441–9.
40. Li C, Vepari C, Jin JH, Kim H, Kaplan D. Electrospun silk-BMP-2 scaffolds for bone tissue engineering. *Biomaterials*. 2006; 27:3115–24.
41. Pham QP, Sharma U, Mikos AG. Electrospun poly(epsilon-caprolactone) microfiber and multilayer nanofiber/microfiber scaffolds: characterization of scaffolds and measurement of cellular infiltration. *Biomacromolecules*. 2006;7:2796–805.